symmetry

MDPI

Article

Effects of Heating Bituminous Mixtures in a Hot-Gas Drum Based on a Finite Volume Method

Xuan Li [1,2,*], Haiying Cheng [1,*], Xiaohui Liu [1] and Wenfeng Zhu [1]

[1] Key Laboratory for Highway Construction Technology and Equipment (Ministry of Education), Chang'an University, Xi'an 710064, China; chd160039@chd.edu.cn (X.L.); zhuwenfeng@chd.edu.cn (W.Z.)
[2] Zhejiang Prulde Electric Appliance Co., Ltd., Jinhua 321000, China
* Correspondence: lxchd@chd.edu.cn (X.L.); chy@chd.edu.cn (H.C.)

Abstract: Hot-gas drum heating (HDH) of bituminous mixtures is a new approach to heating bituminous mixtures that is influenced by the parameters of the hot gas and drum. A fluid thermal numerical model was developed to evaluate the effects of heating bituminous mixtures with HDH using a finite-volume method (FVM). The FVM was verified through the heating test of a bituminous mixture. The effects of the drum rotating speed and hot-gas speed on the efficiency of heating the bituminous mixture during HDH were analyzed using Fluent. The results indicated that the drum rotating speed directly influenced the formation of a bituminous-mixture curtain, which had a significant effect on the efficiency of heating the bituminous mixture. The efficiency of the heat exchange between the hot gas and the bituminous mixture was high, with full contact between the hot gas and the bituminous mixture. With an increase in the hot-gas speed, the heating time became shorter; however, the rate of hot-gas utilization was reduced. A symmetrical temperature distribution and a superior heating efficiency of the bituminous mixture were achieved when the drum rotating speed was 7 rpm and the hot-gas speed was 1.4 m/s.

Keywords: bituminous mixture; hot-gas drum heating; heating effect; finite-volume method; heat transfer

check for updates

Citation: Li, X.; Cheng, H.; Liu, X.; Zhu, W. Effects of Heating Bituminous Mixtures in a Hot-Gas Drum Based on a Finite Volume Method. *Symmetry* **2024**, *16*, 559. https://doi.org/10.3390/sym16050559

Academic Editor: Sorin Vlase

Received: 1 April 2024
Revised: 19 April 2024
Accepted: 23 April 2024
Published: 4 May 2024

1. Introduction

The heating of bituminous mixtures is a necessary process during the hot in-place recycling of asphalt pavements [1,2]. The heating of bituminous mixtures directly influences the construction quality, cost, and efficiency of asphalt pavements [3–5]. Applying superior heating technology has always been the primary goal in asphalt pavement maintenance [6]. Owing to the poor thermal stability of asphalt, the elongation and cohesion of asphalt decrease when the temperature exceeds the aging temperature of asphalt, degrading the performance of the bituminous mixture [7,8]. The conventional heating process of bituminous mixtures consumes a large amount of energy, which leads to severe environmental pollution [9]. The drum heating method is widely applied in the drying of materials and has been used in bituminous mixture heating in recent years [10–12]. The traditional method for heating a bituminous mixture uses heating flues or electrical heat strips, and the bituminous mixture is in a static state in the heating process. The traditional method has a long heating time and a poor temperature distribution symmetry. HDH of bituminous mixtures is a new approach to bituminous mixture heating that can enhance the temperature distribution symmetry in bituminous mixtures, reduce the cost, improve the heating efficiency, and mitigate environmental pollution.

The principle of HDH for bituminous mixtures is shown in Figure 1. Hot gas, which is formed in a hot blast stove with the fuel burning in the burner, flows into the bituminous mixture heating drum. A bituminous-mixture curtain is formed in the drum under the action of a rotating drum and blade, and the bituminous mixture is heated via full contact with a hot gas. The temperature of the hot gas decreases after heat exchange with the bituminous mixture but is still dramatically higher than room temperature. To reduce fuel consumption, most of the hot gas flows into the hot blast stove through a circulating ventilator and is then reheated. The reheated hot gas enters the heating drum, and the bituminous mixture is heated again. A small amount of the hot gas is discharged through the gap between the hot-gas hood and the drum. This cycle is continued until the temperature of the bituminous mixture reaches 160 °C, which is appropriate for construction purposes.

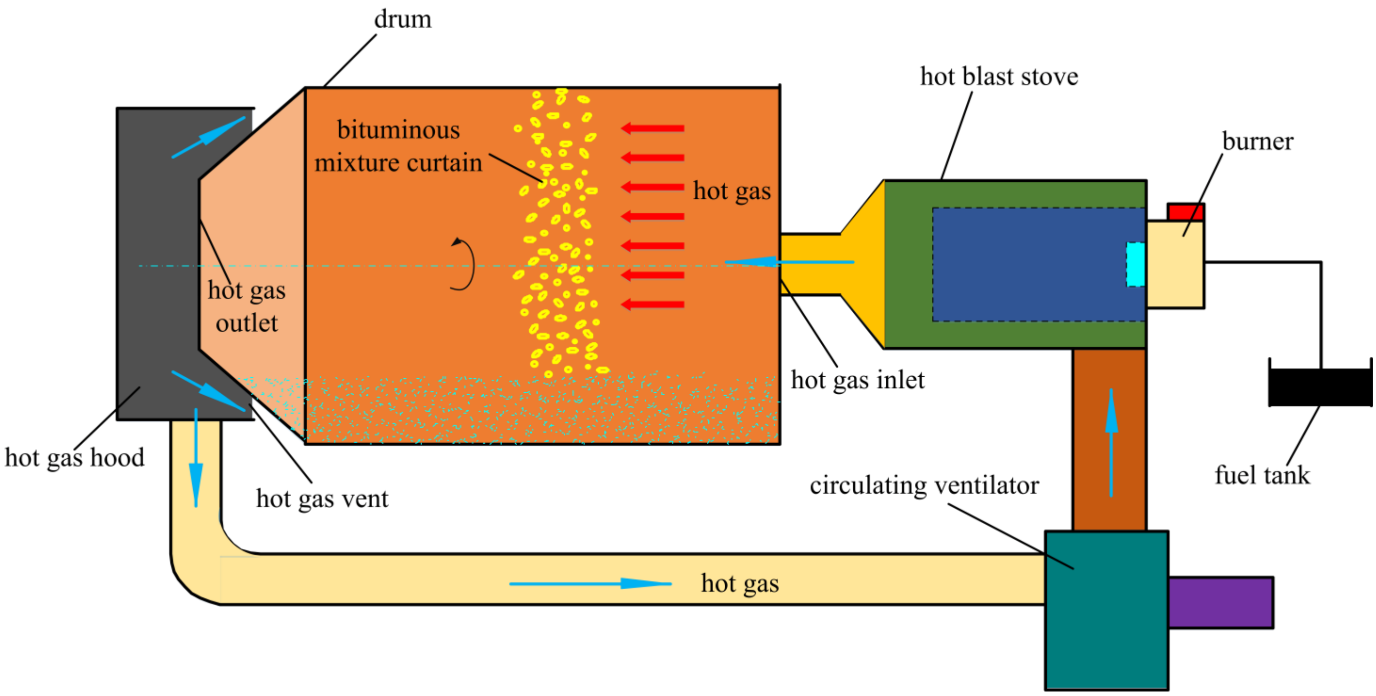

Figure 1. Principles of bituminous mixture heating using HDH.

For the past few years, multiple studies have been conducted on bituminous mixture heating. Chong developed a system of integrated thermodynamic models and a software tool for the estimation of the energy consumption in bituminous mixture production [13]. Ren developed a multiscale model to calculate the effective thermal conductivity of a bituminous mixture according to the principle of minimum thermal resistance [14]. Zhang developed computational models for virtually generating a three-dimensional (3D) random bituminous mixture microstructure and analyzed the thermal conductivity of the heterogeneous microstructure [15]. Wang established a finite-element model for microwave heating of a bituminous mixture to investigate the microwave heating properties of the bituminous mixture [16]. Sarnowski analyzed the properties of non-modified bitumen and SBS polymer-modified bitumen heated at temperatures of 200, 250 and 300 °C for 1 h [17]. Chen analyzed the temperature distribution of porous bituminous mixtures with steel slag aggregates heated by microwaves through laboratory tests and numerical simulations [18]. Ma established a multi-layer low-temperature heat transfer model of bituminous mixtures to study the effects of the multi-layer low-temperature heating method [19]. The above research works offer a reference for the thermal properties of bituminous mixtures. However, little attention has been paid to the heat transfer in the bituminous mixture during HDH. The working parameters of the hot-gas drum are significant factors that affect the heating rate and energy utilization of the bituminous mixture. To gain a better understanding of heat transfer processes in bituminous mixture, it is necessary to study the heating process of bituminous mixtures during HDH.

Numerical studies on engineering practices that are similar to the heating process of bituminous mixtures in a hot-gas drum, such as material drying, material heating, and concrete mixing, are reviewed as follows. Scherer performed coupled discrete element method–computational fluid dynamics (CFD) simulations of the convective drying of wood chips in a baffled laboratory rotary dryer [20]. Zhang reviewed the fundamental thermodynamics and kinematics involved in the production of reclaimed asphalt pavement (RAP) mixtures and the corresponding numerical methodologies to quantify the thermal processes [21]. Xie investigated heat transfer processes in drums with L-shaped lifters by coupling a discrete element method with a heat transfer model [22]. Hanifarianty created a 3D model of a rotary drum dryer including the ambient air to simulate the flow and heat transfer of the rotary drum dryer using CFD [23]. Perarasu simulated the heat transfer of a helical coiled agitated vessel with a varying heat input using CFD [24]. Taghizadeh studied the hydrodynamic behavior of a two-dimensional horizontal rotating drum using the FVM and granular kinetic theory [25]. Zhang investigated the mixing characteristics in a vessel equipped with a cylindrical stirrer in an unbaffled tank and analyzed the flow field, power consumption, and mixing time using CFD [26]. The aforementioned research indicates that CFD may be valid for investigating the flow and heat transfer in bituminous mixtures.

In this study, a numerical simulation of the HDH process of bituminous mixtures was conducted according to the heat transfer principle, hydrodynamic theory, and the FVM. The effects of the drum rotating speed and hot-gas speed on the heating efficiency of bituminous mixtures under HDH were analyzed via Fluent, and the efficiency of hot-gas utilization was examined. The numerical simulation results were compared with the measurement results obtained via experiments to determine the FVM's reliability for analyzing the heating effects of bituminous mixtures under HDH. By applying a proper drum rotating speed and hot-gas speed during HDH, the bituminous mixture heating efficiency and temperature distribution symmetry can be enhanced.

2. Numerical Simulation and Experiment Method

2.1. Finite-Volume Model of Bituminous Mixtures Subjected to HDH

The heating drum consisted of a truncated cone section with a length of 28 cm and a cylindrical section with a length of 1970 mm and a diameter of 1508 mm. To improve the grid quality and calculation accuracy, the truncated cone section was eliminated, considering that the bituminous mixture is mainly contained in the cylindrical section, and a bituminous-mixture curtain was formed in the cylindrical section during heating. The 3D model of HDH is shown in Figure 2a. The blade was L-shaped, its height was 210 mm, and its short-side length was 120 mm. The model was simplified in the numerical simulations, and the drum model in Figure 1 was established and meshed via Gambit. The hot gas parameters were set directly at the drum inlet, and the hot blast stove, burner, fuel tank, and circulating ventilator model in Figure 1 were not established.

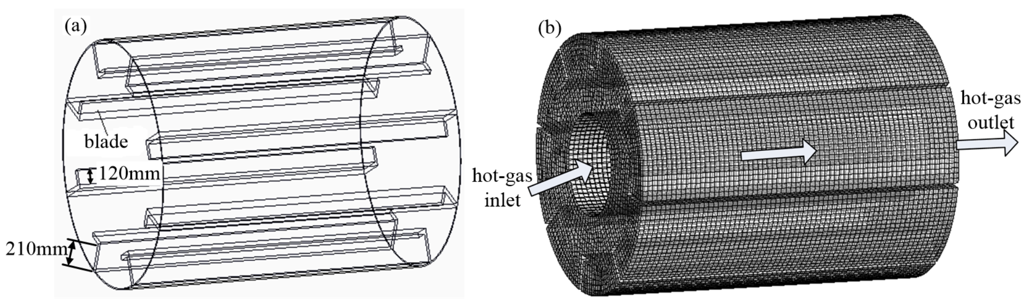

Figure 2. Model of bituminous mixture during HDH: (**a**) 3D perspective of hot gas drum; (**b**) grid model of the bituminous mixture during HDH.

As shown in Figure 2b, the number of grids in the calculated model is 134,426. Further refinement of the grid had a minimal impact on the computational accuracy. The flow-field model can be used to represent the bituminous mixture and hot-gas flow. The hot-gas inlet was a circular surface with a diameter of 600 mm. The hot-gas outlet was on the other side of the drum and was the same size as the hot-gas inlet. The hot-gas inlet was set as the velocity inlet, the hot-gas outlet was set as the outflow. In the flow-field model, the bituminous mixture was defined as an incompressible, non-Newtonian fluid whose dynamic viscosity varies with respect to the temperature [27,28]. A no-slip boundary condition was adopted for the near wall [29,30]. The flows of the bituminous mixture and hot gas were computed using the standard k-ε turbulent model [31]. The Euler multiphase flow model was used for multiphase coupling of the bituminous mixture and hot gas in the drum [32]. The continuity equation for phase q is expressed in Equation (1):

$$\frac{\partial}{\partial t}(\alpha_q \rho_q) + \nabla \cdot \left(\alpha_q \rho_q \vec{v}_q\right) = \sum_{p=1}^{n} \dot{m}_{pq} \tag{1}$$

where α_q is the volume fraction of phase q, ρ_q is the density of phase q, $\vec{v}_q$ is the velocity of phase q, and $\dot{m}_{pq}$ characterizes the mass transfer from phase p to phase q.

The momentum balance for phase q is described by Equation (2)

$$\frac{\partial}{\partial t}\left(\alpha_q \rho_q \vec{v}_q\right) + \nabla \cdot \left(\alpha_q \rho_q \vec{v}_q \vec{v}_q\right) = -\alpha_q \nabla p + \nabla \cdot \overline{\overline{\tau_q}} + \sum_{p=1}^{n}\left(\vec{R}_{pq} + \dot{m}_{pq}\vec{v}_{pq}\right) + \alpha_q \rho_q \left(\vec{F}_q + \vec{F}_{lift,q} + \vec{F}_{Vm,q}\right) \tag{2}$$

where p is the pressure shared by all the phases, $\overline{\overline{\tau_q}}$ is the qth phase stress–strain tensor, $\vec{R}_{pq}$ is the interaction force between the phases, $\vec{v}_{pq}$ is the interphase velocity, $\vec{F}_q$ is the external body force, $\vec{F}_{lift,q}$ is the lift force, and $\vec{F}_{Vm,q}$ is the virtual mass force.

An AC-13C bituminous mixture was taken as the research object. It had a mass of 2 tons, a density of 2450 kg/m^3, a specific heat capacity of 1680 J/(kg·°C), and a thermal conductivity of 3.05 W/(m·K). The air had a density of 1.225 kg/m^3, a specific heat capacity of 1006.43 J/(kg·°C), and a thermal conductivity of 0.0242 W/(m·K) [33]. The temperature of the inlet gas was 400 °C. The bituminous mixture viscosity was defined by a piecewise linear function because it varied with respect to the temperature. The bituminous mixture particles were loose at room temperature (approximately 20 °C). The viscosity coefficient of the bituminous mixture in the FVM model is presented in Table 1 [34]. Considering the insulation of the drum wall, the effect of the heat exchange between the outer wall surface of the drum and the outside was minimal. To reduce the computational complexity, an atmospheric model for the outside of the drum was not established, and the heat exchange between the drum and the atmosphere was neglected. The calculation model of the bituminous mixture under HDH was meshed, and the near-wall grids were refined. In order to ensure the accuracy of the simulation, grid independence was executed. A sliding mesh was used to simulate the bituminous mixture flow and drum rotation, and the drum wall and the blade were set as dynamic boundary conditions. The hot-gas inlet was set as the velocity inlet, and the hot-gas outlet was set as the outlet. Finally, a finite-element thermal and flow-field analysis model based on the finite-element heat conduction equation, standard k-ε turbulent model, and Euler multiphase flow model was established (Figure 2b). The heating of the bituminous mixture was simulated via Fluent.

Table 1. The viscosity coefficient of the AC-13C bituminous mixture at different temperatures.

Temperature (°C)	27	105	120	130	140	160	170
Viscosity (Pa·s)	2.32	1.94	1.15	0.72	0.53	0.2	0.1

2.2. Experimental Method

To verify the numerical model, a hot-gas heating experiment of a bituminous mixture was performed using an asphalt pavement maintenance vehicle (Figure 3a). The asphalt pavement maintenance vehicle was equipped with a temperature monitor and display screen (Figure 3b), which monitored the bituminous mixture's temperature in the drum. The drum rotating speed was 7 rpm, and the drum's structural parameters and the working parameters of the asphalt pavement maintenance vehicle are presented in Table 2.

Figure 3. Heating test of bituminous mixture: (**a**) experimental equipment for heating the bituminous mixture; (**b**) bituminous mixture being heated in the drum; (**c**) heating console and temperature meter of bituminous mixture; (**d**) bituminous mixture after heating.

Table 2. Drum structural and working parameters.

radius of drum	length of drum	wall thickness of drum (with insulating layer)	the short-side length of blade
754 mm	1970 mm	68 mm	120 mm
height of blade	Thickness of blade	hot-air temperature	hot-air flow rate
210 mm	10 mm	400 °C	1.36 m/s

3. Results and Discussion

3.1. Model Verification

To verify the numerical model, the process of heating a bituminous mixture was simulated and experimentally researched. Simulations and experimental tests lasted until the temperature of the bituminous mixture was 160 °C. The temperature of the bituminous mixture was measured each 10 s during simulations, and the bituminous mixture temperature was recorded every 5 min by observing the display screen during the experiment. A comparison of the experimental results with the simulation results of the bituminous mixture using HDH is presented in Figure 4.

As indicated by Figure 4, the starting temperature of the bituminous mixture was 16 °C, and the time taken to heat the mixture to 160 °C was 1980s in the experiment. The similarity between the simulation results and the test results indicates that the simulation results correctly reflect the temperature variation of the bituminous mixture during heating. However, there was a difference between the experimental and simulation results for the temperature variation of the bituminous mixture under HDH. The reason for this difference is that the initial temperature of the bituminous mixture was lower in the experiment and part of the heat was lost during actual heating. The drum was considered to be adiabatic (i.e., there was no heat exchange between the drum and the external environment). Consequently, the heating time of bituminous mixture was longer in the experiment compared with the simulation.

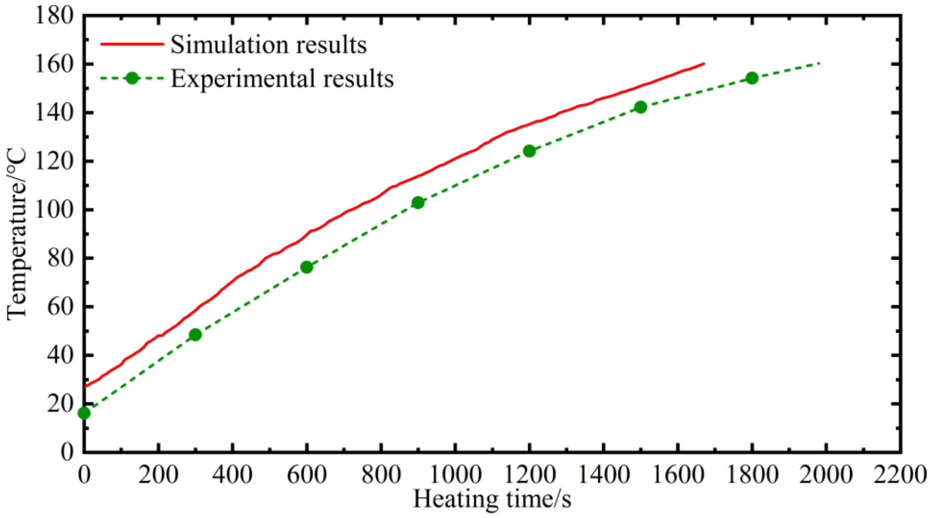

Figure 4. Comparison between experiment and numerical simulation of bituminous mixture heating.

In the experiment, the bituminous mixture was discharged from the drum when the temperature reached 160 °C. The temperature was measured using a UT322 thermometer. It was impossible to selecting the same measurement points in the experiment and numerical simulations. However, the temperature at random monitoring points can truly reflect the temperature of asphalt mixtures. It is feasible to verify the reliability of the model by comparing the bituminous mixture's temperature at random monitoring points throughout the numerical simulation and experiment. Ten random monitoring points for the bituminous mixture were selected. The experimental and simulation results are presented in Figure 5. As shown, the maximum temperature gap between the monitoring points of the bituminous mixture was approximately 4 °C, indicating that the temperature of the bituminous mixture was uniform under HDH. The temperature differences between the monitoring points of the bituminous mixture were slightly smaller in the simulation than in the experiment. Excellent agreement was observed between the simulation and experimental results.

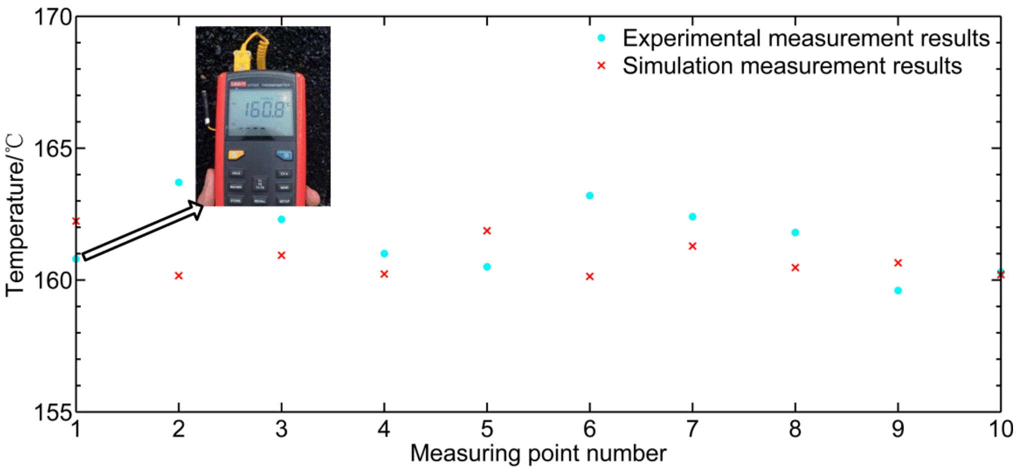

Figure 5. Numerical simulation results and experimental verification.

3.2. Effect of the Drum's Rotating Speed on the Heating Efficiency of Bituminous Mixtures

The effect of the drum rotating speed on the heating efficiency of the bituminous mixtures was examined when the speed of the hot gas was 1.36 m/s. The bituminous mixture was heated to 160 °C, and the temperature field of the bituminous mixture was analyzed at 160 °C. When the drum rotating speed is 7 rpm and the hot-gas speed is 1.36 m/s, the temperature distribution of the bituminous mixture in the drum, including the transverse cross-section and longitudinal cross-section, under HDH is depicted in Figure 6.

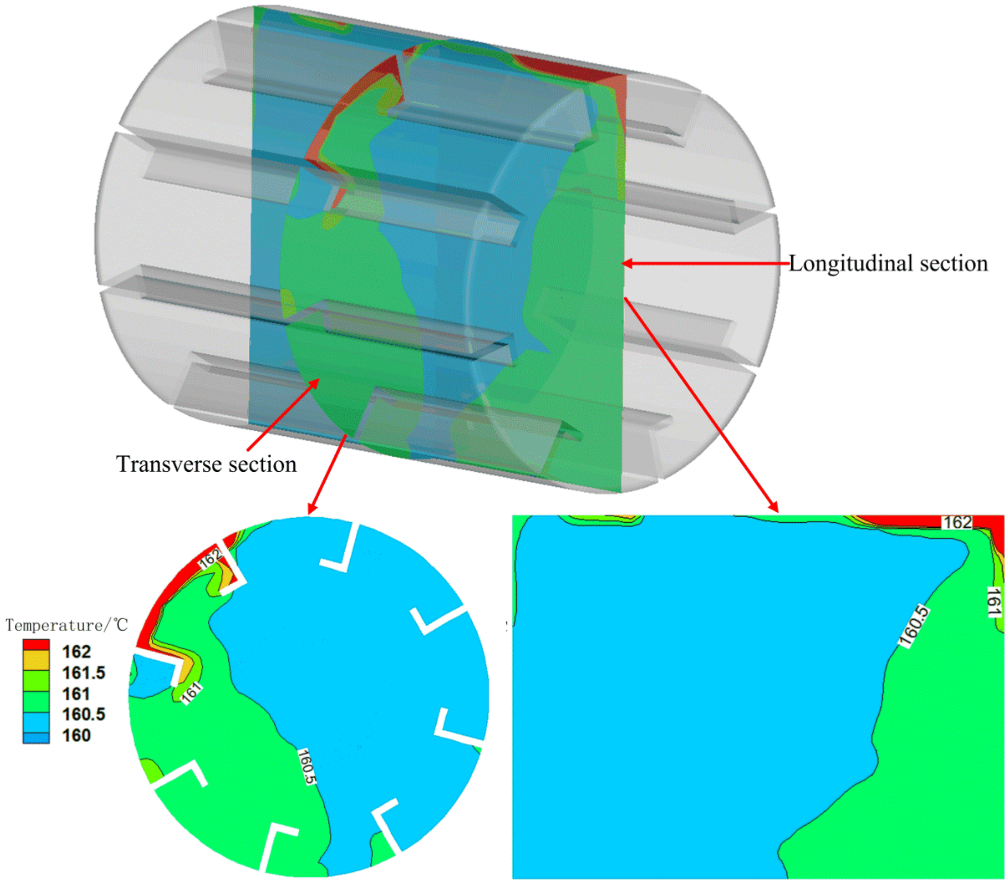

Figure 6. Temperature distributions of the bituminous mixture during HDH.

As shown in Figure 6, the temperature of the bituminous mixture in the drum ranged between 160.5 and 161 °C. This indicates that there was nearly no temperature difference in the bituminous mixture using HDH. The temperature in the red area above the drum was higher, as a small part of the bituminous mixture adhered to the drum wall and the blade. The temperature of this part of the bituminous mixture exceeded 162 °C due to hot-gas heat transfer and the high-temperature drum wall. The proportion of the bituminous mixture adhering to the drum wall and the blade was small, and this does not indicate uneven heating of the bituminous mixture.

The minimum temperature of the bituminous mixture was monitored during the simulation until it reached 160 °C, and the temperature variation of the bituminous mixture at the monitoring point was determined. The temperature variations of the bituminous mixture at different drum rotating speeds are shown in Figure 7. The heating periods of the bituminous mixture for various drum rotating speeds are shown in Figure 8, under the condition of identical working parameters, and the bituminous mixture was heated to 160 °C (note that the minimum temperature of the bituminous mixture reached 160 °C).

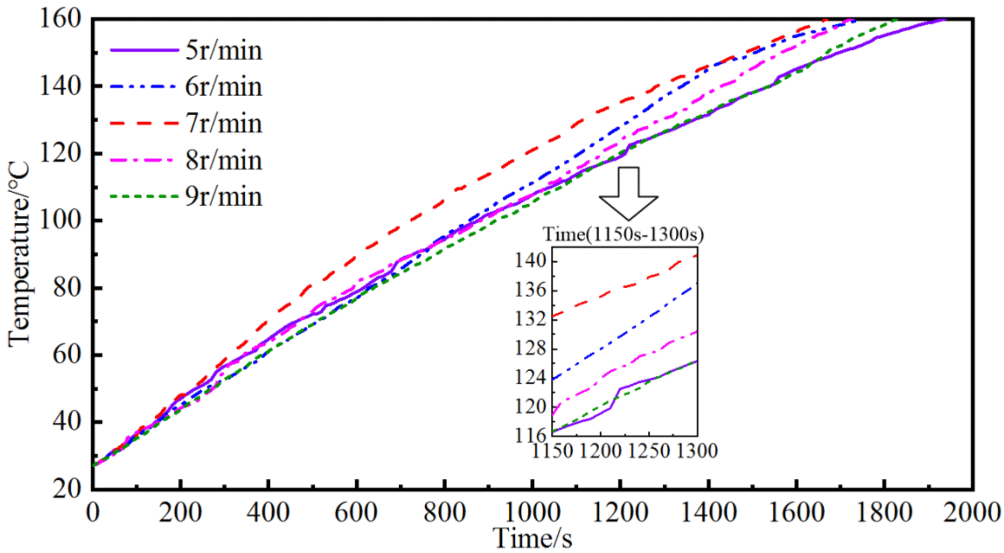

Figure 7. Temperature variation of the bituminous mixture during HDH with different drum rotating speeds.

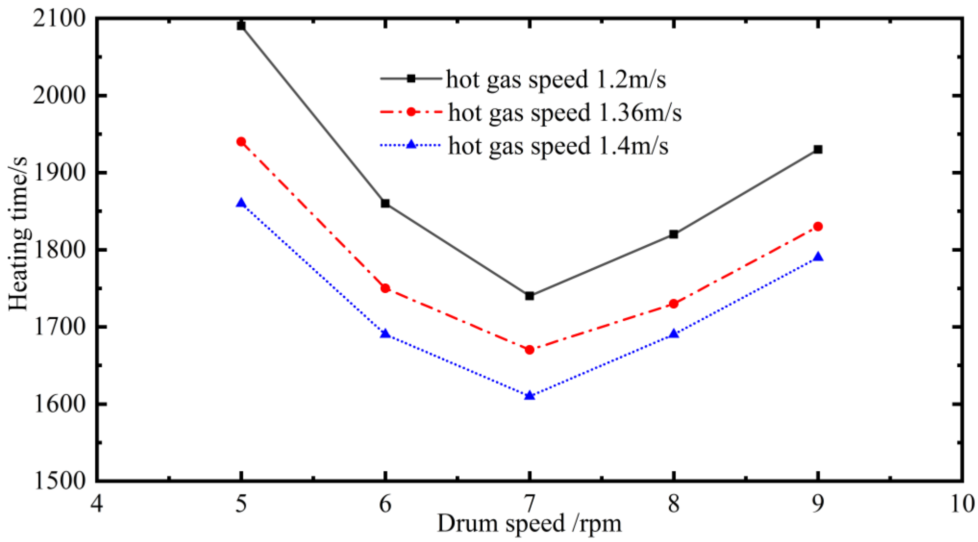

Figure 8. Heating time of the bituminous mixture heated to 160 °C for different drum rotating speeds at a hot-gas speed of 1.2, 1.36 and 1.4 m/s.

As shown in Figure 7, the slope of the curve of the temperature of the bituminous mixture was steep during the starting period and gradually decreased over time. This implies that the bituminous mixture's temperature increased rapidly at the beginning and then increased gradually with the heating time. When the bituminous mixture's temperature was low, the temperature gap between the hot gas and the mixture was large. The heat-transfer efficiency between the bituminous mixture and hot gas was initially high, and the temperature of the bituminous mixture increased rapidly. The temperature gap between the bituminous mixture and the hot gas gradually decreased with the increase in the bituminous mixture's temperature, and the heat-transfer rate decreased. Therefore, the rate of the temperature rise of the bituminous mixture decreased.

As shown in Figure 7, there were several "small steps" in the temperature curve of the bituminous mixture when the drum rotating speed was 5 rpm. These "steps" indicate that the temperature rise of the bituminous mixture was sometimes rapid or slow because of the intermittent formation of a mixture curtain. The temperature of the bituminous mixture increased rapidly when the curtain was fully formed but increased slowly when the curtain was not completely formed or not formed at all. The temperature curve of the bituminous mixture was relatively stable, and there were hardly any "small steps" in the curve when the drum rotating speed was 7, 8 and 9 rpm because the mixture curtain was stable at higher drum rotating speeds.

As shown in Figure 8, when the drum moved at a lower rotational speed, the heating time of the bituminous mixture was longer and the heating efficiency was lower. This trend occurred because the lifting of the bituminous mixture by the blade was too slow, and the mixture curtain sometimes disappeared when the drum moved at a low rotational speed. Additionally, the efficiency of the heat exchange between the hot gas and the bituminous mixture was significantly reduced when there was no full contact with the bituminous mixture, which resulted in a longer heating time of the bituminous mixture. Furthermore, the heating efficiency of the bituminous mixture was low when the drum rotating speed was very high. This is because part of the bituminous mixture rotated with the drum without falling. Although a mixture curtain was formed continuously, its area was small, and the heat exchange efficiency between the hot gas and bituminous mixture was low with a small contact area. Furthermore, the heating time was the shortest when the drum rotating speed is 7 rpm at hot-gas speeds of 1.2, 1.36 and 1.4 m/s.

Various pieces of evidence indicate that both higher and lower drum rotating speeds adversely affect the heating of the bituminous mixture. The lifting of the bituminous mixture by the blade was not quick enough, and the mixture curtain sometimes disappeared at a low drum rotating speed. The utilization of hot gas was reduced, resulting in a low efficiency of bituminous mixture heating. Although a mixture curtain was formed continuously, the formed bituminous-mixture curtain area was small because part of the bituminous mixture rotated with the drum without falling when the drum rotating speed was very high. Consequently, the heating efficiency of the bituminous mixture was low. The heating efficiency of the bituminous mixture was higher when the drum rotating speed was 7 rpm. Therefore, it is appropriate to set the drum rotating speed to 7 rpm.

3.3. Effect of Hot-Gas Speed on the Heating Efficiency of the Bituminous Mixture

The hot-gas speed is a critical parameter for bituminous mixtures with hot-gas heating. To determine an adequate hot-gas speed, the effects of the hot-gas speed on the bituminous-mixture heating efficiency and the efficiency of hot-gas utilization at a drum rotating speed of 7 rpm were investigated.

The heating period and hot-gas consumption of the bituminous mixture under HDH for different hot-gas speeds are presented in Figure 9. As shown, the hot-gas speed significantly affected the heating period of the bituminous mixture. The heating period of the bituminous mixture decreased with an increase in the hot-gas speed. A higher speed corresponded to a shorter heating time of the bituminous mixture, although the efficiency of heat utilization was reduced. Although part of the hot gas was recycled and reused after heating the bituminous mixture, some of the hot gas was lost in the heating process, and a large amount of energy was consumed. Moreover, when the hot-gas speed reached a certain value, the heating-up period of the mixture was not significantly shortened with the increase in hot-gas speed. In contrast, at a high hot-gas speed, the heating-up period of the bituminous mixture was short, but the hot-gas consumption increased, and more energy was wasted. The above analysis indicates that the hot-gas speed should neither be very low nor very high. When the hot-gas speed was increased from 1.2 to 1.4 m/s, the heating-up period of the bituminous mixture was significantly shortened, and the hot-gas consumption increased slightly. Therefore, it is suitable to set the hot-gas speed to 1.4 m/s.

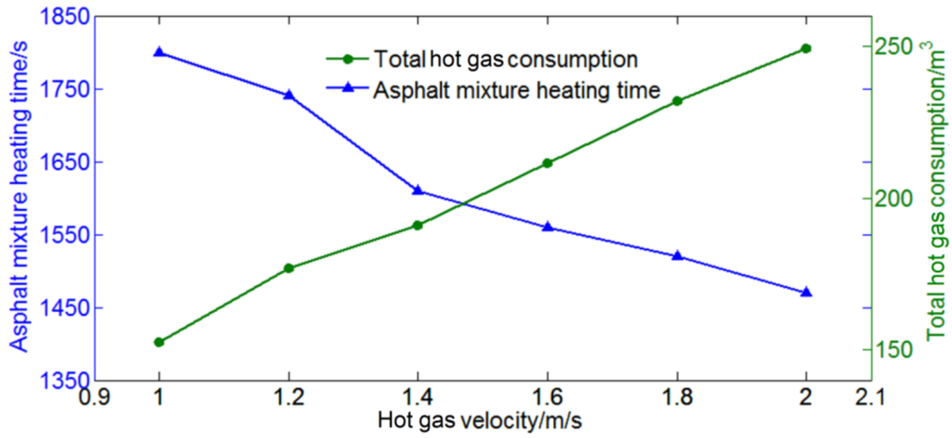

Figure 9. Heating time and hot-gas consumption of the bituminous mixture during HDH.

3.4. Hot-Gas Temperature at the Drum Outlet

To further investigate the heating effect, the hot-gas temperature at the drum outlet was monitored in the simulation, and the area-weighted mean of the hot-gas temperature at the drum outlet was calculated. The variations in the hot-gas temperature at the drum outlet with different drum rotating speeds are presented in Figure 10.

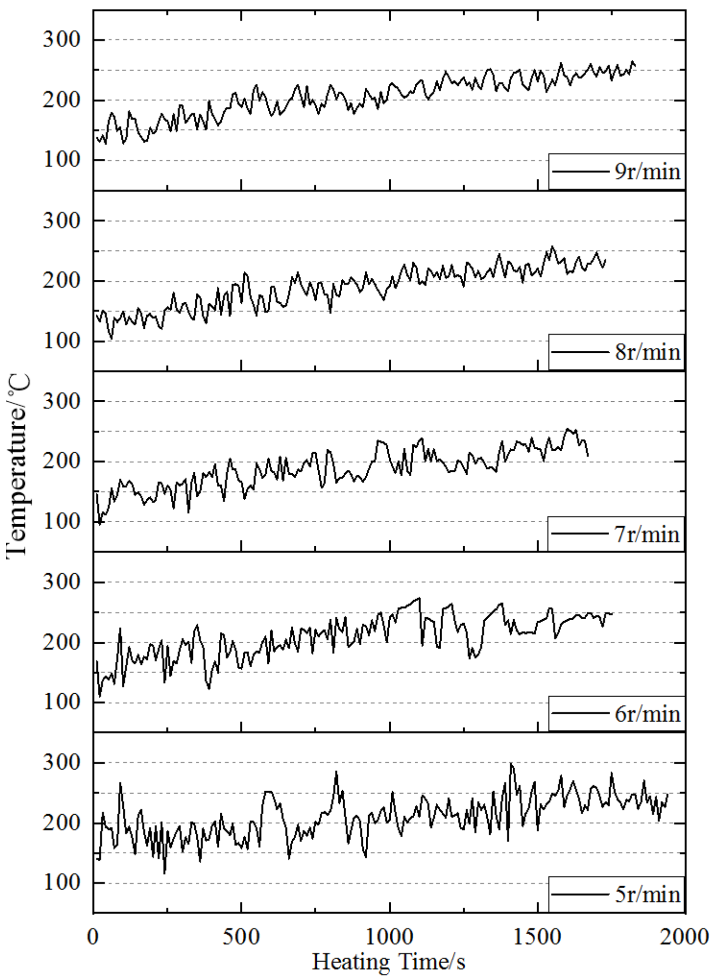

Figure 10. Temperature variation of hot gas at the drum outlet with different drum rotating speeds.

In Figure 10, the hot-gas temperature fluctuation at the drum outlet is significant. The reason for this fluctuation is that the bituminous-mixture curtain forming in the drum was unstable. When the formed bituminous-mixture curtain area was large, heat exchange between the hot gas and the bituminous mixture was sufficient, and the hot-gas temperature of the drum outlet was low. When the formed bituminous-mixture curtain area was smaller, the amount of heat exchanged was lower and the hot-gas temperature at the drum outlet was higher. Owing to the intermittent curtain formation in the bituminous mixture at a low drum rotating speed, the hot-gas temperature of the drum outlet fluctuated significantly when the drum rotating speed was 5 rpm. With an increase in the drum rotating speed, the instability of the bituminous-mixture curtain steadily decreased and a bituminous-mixture curtain was formed continuously. Therefore, the temperature fluctuation of the hot gas at the drum outlet gradually decreased. Furthermore, the hot-gas temperature ay the drum outlet gradually increased during the heating process. With an increase in the bituminous mixture's temperature, the amount of heat exchange between the bituminous mixture and the hot gas decreased, and the reduction in the temperature of the hot gas was mitigated.

4. Conclusions

The heat transfer and mechanisms of bituminous mixtures during HDH were investigated. FVM-based numerical models were constructed on the basis of the bituminous mixture parameters, such as the gradation, thermal conductivity, specific heat capacity, and viscosity coefficient, and then verified. The proposed method is a viable approach for studying the effects of heating bituminous mixtures under different conditions. The following conclusions are drawn:

(1) The simulation results obtained using an FVM are in agreement with the tests, indicating that the simulation method can predict the temperature variation of a bituminous mixture during heating. It is concluded that the FVM can be used to evaluate the effects of heating bituminous mixtures and optimize the operating parameters of HDH equipment.

(2) In the simulation results, the slope of the bituminous mixture's temperature curve is steep during the initial period and gradually decreases over time. The temperature gap between the bituminous mixture and the hot gas gradually decreases with an increase in the bituminous mixture's temperature. Consequently, the heat-exchange rate decreases and the temperature increase in the bituminous mixture slows down.

(3) Excessively high or low drum rotating speeds are not conductive to the formation of a bituminous-mixture curtain, which affects the efficiency of the heat exchange between the hot gas and the bituminous mixture. The amount of heat exchanged increases with the bituminous-mixture curtain area. For the simulations with drum rotating speeds of around 5, 6, 7, 8 and 9 rpm, the heating time is 1940, 1750, 1670, 1730, and 1830s. The heating time is the shortest when the drum speed is 7 rpm.

(4) The hot-gas speed significantly affects the heating rate of the bituminous mixture. With an increase in the hot-gas speed, the heating time of the bituminous mixture is shortened, but the efficiency of hot-gas heat utilization is reduced. According to a comprehensive analysis of the hot-gas consumption and heating efficiency, when the hot-gas speed is increased from 1.2 to 1.4 m/s, the bituminous mixture's heating-up period is significantly reduced and the hot-gas consumption is increased slightly. Therefore, it is suitable to set the hot-gas speed to 1.4 m/s.

(5) The hot-gas temperature fluctuation at the drum outlet is significant, as the bituminous-mixture curtain forming in the drum is unstable. The temperature fluctuation of the hot gas at the drum outlet was observed to decrease with an increase in the drum rotating speed, as the formation of a bituminous-mixture curtain is more continuous if the drum rotating speed is high. Although the temperature fluctuation of the hot gas at the drum outlet is small, the average temperature of the hot gas is higher when the drum speed is higher. When the drum rotating speed is 7 rpm, the average temperature of the hot gas at the drum outlet is lower, indicating a higher hot-gas utilization rate and a higher mixture heating efficiency.

Author Contributions: Conceptualization, X.L. (Xuan Li) and H.C.; methodology, X.L. (Xuan Li); validation, X.L. (Xuan Li) and W.Z.; formal analysis, X.L. (Xiaohui Liu); investigation, X.L. (Xuan Li); resources, H.C.; data curation, X.L. (Xuan Li); writing—original draft preparation, X.L. (Xuan Li); writing—review and editing, X.L. (Xuan Li) and H.C.; visualization, X.L. (Xuan Li). All authors have read and agreed to the published version of the manuscript.

Funding: This research was supported by National Natural Science Foundation of China (project Nos. 52375230, 52375080) and the Natural Science Basic Research Plan of Shaanxi (Nos. 2022JZ26, 2023JCQN0472, 2024JCYBMS413).

Data Availability Statement: Data are contained within the article.

Conflicts of Interest: Author Xuan Li was employed by the Zhejiang Prulde Electric Appliance Co., Ltd. The remaining authors declare that the research was conducted in the absence of any commercial or financial relationship that could be construed as a potential conflict of interest.

References

1. Liu, Y.; Wang, H.N.; Tighe, S.L.; Zhao, G.Y.; You, Z.P. Effects of preheating conditions on performance and workability of hot in-place recycled asphalt mixtures. *Constr. Build. Mater.* **2019**, *226*, 288–298. [CrossRef]
2. Zhu, Y.J.; Ma, T.; Xu, G.J.; Fan, J.W.; Zhang, Y.M. Study of the mixing between asphalt and rejuvenator in hot in-place recycled layer. *J. Transp. Eng. B-Pavements* **2023**, *149*, 04023005. [CrossRef]
3. Xu, X.X.; Gu, H.R.; Dong, Q.Z.; Li, J.P.; Jiao, S.J.; Ren, J. Quick heating method of asphalt pavement in hot in-place recycling. *Constr. Build. Mater.* **2018**, *178*, 211–218. [CrossRef]
4. Bouraima, M.B.; Zhang, X.H.; Rahman, A.; Qiu, Y.J. A comparative study on asphalt binder and mixture performance of two traffic lanes during hot in-place recycling (HIR) procedure. *Constr. Build. Mater.* **2019**, *223*, 33–431. [CrossRef]
5. Chen, Y.H.; Chen, Z.G.; Xiang, Q.; Qin, W.J.; Yi, J.Y. Research on the influence of RAP and aged asphalt on the performance of plant-mixed hot recycled asphalt mixture and blended asphalt. *Case Stud. Constr. Mater.* **2021**, *15*, e00722. [CrossRef]
6. Pan, Y.Y.; Liu, G.Q.; Tang, D.; Han, D.D.; Li, X.G.; Zhao, Y.L. A rutting-based optimum maintenance decision strategy of hot in-place recycling in semi-rigid base asphalt pavement. *J. Clean. Prod.* **2021**, *297*, 126663. [CrossRef]
7. Yuan, Y.; Zhu, X.; Chen, L. Relationship among cohesion, adhesion, and bond strength: From multi-scale investigation of asphalt-based composites subjected to laboratory-simulated aging. *Mater. Des.* **2020**, *185*, 108272. [CrossRef]
8. Gu, H.R.; Xu, X.X.; Xiao, R.; Qi, B.Y.; Jiang, Z.C. Multi-stage heating technology for asphalt pavement hot in-place recycling using controlled heating power. *Int. J. Pavement Eng.* **2023**, *24*, 2199993. [CrossRef]
9. Thives, L.P.; Ghisi, E. Asphalt mixtures emission and energy consumption: A review. *Renew. Sustain. Energy Rev.* **2017**, *72*, 473–484. [CrossRef]
10. Firouzi, S.; Alizadeh, M.R.; Haghtalab, D. Energy consumption and rice milling quality upon drying paddy with a newly-designed horizontal rotary dryer. *Energy* **2017**, *119*, 629–636. [CrossRef]
11. Shao, H.J.; Sun, L.J.; Liu, L.P.; You, Z.P.; Yang, X. A novel double-drum mixing technique for plant hot mix asphalt recycling with high reclaimed asphalt pavement content and rejuvenator. *Constr. Build. Mater.* **2017**, *134*, 236–244. [CrossRef]
12. Alit, I.B.; Susana, I.G.B.; Mara, I.M. Thermal characteristics of the dryer with rice husk double furnace—Heat exchanger for smallholder scale drying. *Case Stud. Therm. Eng.* **2021**, *28*, 101565. [CrossRef]
13. Chong, D.; Wang, Y.H.; Chen, L.; Yu, B. Modeling and validation of energy consumption in asphalt mixture production. *J. Constr. Eng. Manag.* **2016**, *142*, 04016069. [CrossRef]
14. Ren, Z.S.; Wang, H.; Zhang, L.; Chen, C.X. Computational analysis of thermal conductivity of asphalt mixture based on a multiscale mathematical model. *J. Eng. Mech.* **2018**, *144*, 04018064. [CrossRef]
15. Zhang, L.; Wang, H.; Ren, Z.S. Computational analysis of thermal conductivity of asphalt mixture using virtually generated three-dimensional microstructure. *J. Mater. Civ. Eng.* **2017**, *29*, 04017234. [CrossRef]
16. Wang, H.P.; Zhang, Y.; Zhang, Y.; Feng, S.Y.; Lu, G.Y.; Cao, L.T. Laboratory and numerical investigation of microwave heating properties of asphalt mixture. *Materials* **2019**, *12*, 146. [CrossRef]
17. Sarnowski, M.; Kowalski, K.J.; Król, J.B.; Radziszewski, P. Influence of overheating phenomenon on bitumen and asphalt mixture properties. *Materials* **2019**, *12*, 610. [CrossRef]
18. Chen, X.Q.; Wang, Y.H.; Liu, Z.H.; Dong, Q.; Zhao, X.K. Temperature analyses of porous asphalt mixture using steel slag aggregates heated by microwave through laboratory tests and numerical simulations. *J. Clean. Prod.* **2022**, *338*, 130614. [CrossRef]
19. Ma, D.C.; Lan, F. Numerical simulation analysis on multi-layer low-temperature heating method of asphalt pavement in hot in-place recycling. *J. Cent. South Univ.* **2021**, *27*, 3793–3806. [CrossRef]
20. Scherer, V.; Mönnigmann, M.; Berner, M.O.; Sudbrock, F. Coupled DEM–CFD simulation of drying wood chips in a rotary drum–baffle design and model reduction. *Fuel* **2016**, *184*, 896–904. [CrossRef]
21. Zhang, K.; Huchet, F.; Hobbs, A. A review of thermal processes in the production and their influences on performance of asphalt mixtures with reclaimed asphalt pavement (RAP). *Constr. Build. Mater.* **2019**, *206*, 609–619. [CrossRef]

22. Xie, Q.; Chen, Z.; Mao, Y. Case studies of heat conduction in rotary drums with L-shaped lifters via DEM. *Case Stud. Therm. Eng.* **2018**, *11*, 145–152. [CrossRef]
23. Hanifarianty, S.; Legwiriyakul, A.; Alimalbari, A.; Nuntadusit, T. A rotary drum dryer for palm sterilization: Preliminary study of flow and heat transfer using CFD. *IOP Conf. Ser. Mater. Sci. Eng.* **2018**, *297*, 012030. [CrossRef]
24. Perarasu, V.T.; Arivazhagan, M.; Sivashanmugam, P. CFD modelling study of heat transfer in a coiled agitated vessel. *Prog. Comput. Fluid Dyn.* **2014**, *14*, 177–188. [CrossRef]
25. Taghizadeh, A.; Hashemabadi, S.H.; Yazdani, E.; Akbari, S. Numerical analysis of restitution coefficient, rotational speed and particle size effects on the hydrodynamics of particles in a rotating drum. *Granul. Matter* **2018**, *20*, 1–13. [CrossRef]
26. Zhang, P.; Chen, G.; Duan, J.; Wang, W.W. Mixing characteristics in a vessel equipped with cylindrical stirrer. *Results Phys.* **2018**, *10*, 699–705. [CrossRef]
27. Mousazadeh, F.; Akker, H.E.A.V.D.; Mudde, R.F. Eulerian simulation of heat transfer in a trickle bed reactor with constant wall temperature. *Chem. Eng. J.* **2012**, *207*, 675–682. [CrossRef]
28. Ershadnia, R.; Amooie, M.A.; Shams, R.; Hajirezaie, S.; Liu, Y.H.; Jamshidi, S.; Soltanian, M.R. Non-Newtonian fluid flow dynamics in rotating annular media: Physics-based and data-driven modeling. *J. Pet. Sci. Eng.* **2020**, *11*, 106641. [CrossRef]
29. Machado, M.V.C.; Nascimento, S.M.; Duarte, C.R.; Barrozo, M.A. Boundary conditions effects on the particle dynamic flow in a rotary drum with a single flight. *Powder Technol.* **2017**, *311*, 341–349. [CrossRef]
30. Delele, M.A.; Weigler, F.; Franke, G.; Mellmann, J. Studying the solids and fluid flow behavior in rotary drums based on a multiphase CFD model. *Powder Technol.* **2016**, *292*, 260–271. [CrossRef]
31. Sun, Z.; Zhu, H.; Hua, J. Granular flow characteristics and heat generation mechanisms in an agitating drum with sphere particles: Numerical modeling and experiments. *Powder Technol.* **2018**, *339*, 149–166. [CrossRef]
32. Parsi, M.; Kara, M.; Agrawal, M.; Kesana, N.; Jatale, A.; Sharma, P.; Shirazi, S. CFD simulation of sand particle erosion under multiphase flow conditions. *Wear* **2017**, *376*, 1176–1184. [CrossRef]
33. Hassn, A.; Chiarelli, A.; Dawson, A.; Garcia, A. Thermal properties of asphalt pavements under dry and wet conditions. *Mater. Des.* **2016**, *91*, 432–439. [CrossRef]
34. Luo, Y.F.; Zhang, K.; Li, P.L.; Yang, J.H.; Xie, X.B. Performance evaluation of stone mastic asphalt mixture with different high viscosity modified asphalt based on laboratory tests. *Constr. Build. Mater.* **2019**, *225*, 214–222. [CrossRef]